Maser effect due to thermal excitation of the spin system in a paramagnetic crystal by a pulsed magnetic field

M. P. Vaĭsfel'd, F. S. Imamutdinov, and A. Kh. Khasanov

Kazan' University; Kazan' Aviation Institute

(Submitted 25 October 1982)
Zh. Eksp. Teor. Fiz. **84**, 2168–2179 (June 1983)

The maser effect on spin sublevels of $^{59}Co^{2+}$ ions in the $^{59}Co^{2+}$:Ce^{3+}:$La_2Mg_3(NO_3)_{12}24H_2O$ crystal is investigated experimentally and theoretically in the three-centimeter range. In contrast to paramagnetic amplifiers with microwave or optical pumping, quantum amplification was effected directly at the expense of the energy of thermal phonons of the crystal immersed in liquid helium. The EPR spectrum and the kinetics of the spectral transitions of the Co^{2+} ions are studied under thermal excitation conditions. The main kinetic and thermodynamic parameters of the spin system are determined.

PACS numbers: 42.52. + x, 78.70.Gq, 76.30.Fc 75.20.Ck

INTRODUCTION

In 1960, Scovil and Shulz-Du Bois[1], starting from the fundamental analogy[2] between masers and heat engines, indicated that states with negative spin temperature can be obtained in a paramagnetic crystal exclusively on account of thermal excitation of system. They have proposed[3,4] a ruby maser system excited by adiabatic fast (relative to the Cr^{3+} spins) cooling of a pre-heated crystal lattice. Basov and Oraevskiĭ[5] analyzed the thermal method of exciting states with negative temperature from general theoretical points of view and described the conditions for their onset in a three-level system. Subsequently, the development of the ideas connected with the thermal method has let to the creation of gasdynamic lasers (GDL).[6,7] In devices of this type it was possible to obtain, for the first time, direct conversion of the energy of a heated body (gas) into coherent IR-radiation energy. The GDL is the first embodiment of the basic premises of the concept of quantum heat engine,[2,8] discussed in the methodologically important article of Konyukhov and Prokhorov.[4]

Successful realization of the thermal method in mixtures of molecular gases that are the working media of GDL has stimulated a search for new ways of realizing the principle of thermal excitation in condensed media. One variant of the solution of this problem in the microwave band was developed theoretically in Refs. 9 and 10, where, for crystals of the binary lanthanum magnesium nitrate (LaMN) type, with CO^{2+} and Ce^{3+} as impurities, it was shown that after deep cooling of the spins of the Ce^{3+} by adiabatic demagnetization, the interaction of the latter with the nuclear spins of Co^{59} can lead, under certain conditions, to partial inversion of the populations in the spin-sublevel system of cobalt. This effect was subsequently confirmed by experiment.[11] In this article we present the results of a detailed investigation of a thermal maser based on $^{59}Co^{2+}$:Ce^{3+}:LaMN.

1. METHOD OF OBTAINING INVERTED POPULATION

In the method described we use the features of the spectral and relaxation characteristics of Co^{2+} and C^{3+} in the LaMN crystal.[9–16] In this compound, the Co^{2+} ions can occupy two magnetically nonequivalent positions, X and Y. In both cases, the spin Hamiltonian in the magnetic field H takes the form ($S = 1/2$, $I = 7/2$) (Refs. 9 and 12)

$$\hat{\mathcal{H}}_A = g_{\parallel}^{A}\beta H_z\hat{S}_z + g_{\perp}^{A}\beta(H_x\hat{S}_x + H_y\hat{S}_y) + A_{\parallel}\hat{S}_z\hat{I}_z + A_{\perp}(\hat{S}_x\hat{I}_x + \hat{S}_y\hat{I}_y) - g_{\parallel}^{N}\beta_N H_z\hat{I}_z - g_{\perp}^{N}\beta_N(H_x\hat{I}_x + H_y\hat{I}_y) + P_{\parallel}[\hat{I}_z^2 - {}^1/_3 I(I+1)], \quad (1)$$

where the z axis is taken to be the direction of the C_3 axis of the crystal; all the notation in (1) is standard.[13] For the X centers of CO^{2+} the ENDOR method yielded[12] the spin-Hamiltonian parameters $g_{\parallel}^{A} = 4.043$, $g_{\perp}^{A} = 4.432$, $A_{\parallel} = 79.096\cdot10^{-4}$ cm^{-1}, $A_{\perp} = 103.911\cdot10^{-4}$ cm^{-1}, $g_{\perp}^{N} = 1.854$, $g_{\perp}^{N} = 1.897$, and $P_{\parallel} = 0.0720\cdot10^{-4}$ cm^{-1}.

The eigenvalues $E^A(M,m)$ of the Hamiltonian $\hat{\mathcal{H}}_A$ can be obtained by perturbation theory[9,13]:

$$E_A(M, m) = \delta M + AMm + E_A'(M, m). \quad (2)$$

Here M and m are the electron and spin quantum numbers ($M = \pm 1/2$, $-I \leqslant m \leqslant I$), $\delta = g_A(\theta)\beta H$ is the electron Zeeman splitting (θ is the angle between the vector **H** and the C_3 axis), $A = A(\theta)$ is the hyperfine structure (hfs) constant in the field **H**, and $E_A'(M,m)$ characterizes the contributions of second order of smallness; explicit expressions for δ, A, and $E_A'(M,m)$ are given in Ref. 9.

From the data of our measurements, performed on an LaMN:0.1 at.%Co^{2+} sample by the method of pulsed EPR saturation ($\nu = 9.3$ GHz at temperatures below 2 K and spin-lattice relaxation (SLR) of Co^{2+}, a direct process predominates, and the main contribution is made by the transitions $1/2, m \leftrightarrow -1/2, m$. At a lattice temperature $T_L = 1.7$ K in a field $\mathbf{H} \| C_3$, the corresponding rates are $T_A^{-1}(m) \sim 10$ sec^{-1}.

The spin-Hamiltonian of the Ce^{2+} ions is of the form[9,12] ($J = 1/2$)

$$\hat{\mathcal{H}}_B = g_{\parallel}^{B}\beta H_z\hat{J}_z + g_{\perp}^{B}\beta(H_x\hat{J}_x + H_y\hat{J}_y), \quad (3)$$

and the g factor is strongly anisotropic: $g_{\parallel}^{B} = 0.0235$, $g_{\perp}^{B} = 1.8264$.[12] Our measurements, performed in a 0.1 at.% Co^{2+} :3 at.% Ce^{3+}:LaMN sample at a temperature

 0038-5646/83/061263-07$04.00 © 1984 American Institute of Physics

$T_L = 1.7$ K and a frequency $= 9.1$ GHz in a field $\mathbf{H} \| C_3$ yielded for the time T_B of the SLR of Ce^{3+} a value 15 msec.

Most important is following property of the considered spin system. In a wide range of fields, $H_0 \leqslant A_\parallel / 2g_\parallel^B \beta$, it is possible to satisfy the condition of electron-nuclear cross relaxation (ENCR) between the spins of Ce^{3+} and the nuclear spins of Co^{59}:

$$^1/_2 A(\theta_0) = \delta_B(\mathbf{H}_0) = \beta H_0 [(g_\parallel^B \cos\theta_0)^2 + (g_\perp^B \sin\theta_0)^2]^{1/2}. \quad (4)$$

Here $\delta_B(\mathbf{H}_0)$ is the Zeeman splitting of the levels $M_J = \pm(1/2)$ Ce^{3+} in the field $\mathbf{H}_0$, and θ_0 is the angle between the vector $\mathbf{H}_0$ and the C_3 axis.

In this system, states with inverted population of the spin sublevels of cobalt can be obtained in the following manner. A static magnetic field H_0 is applied to the crystal cooled to a temperature $T_L \lesssim 2$ K. The magnitude and direction of the field are chosen to satisfy the condition (4) and to have the splitting δ in (2) land in the frequency range of the EPR spectrometer. It is assumed that the density n_B of the Ce^{3+} ions in the sample is such that the following relations are satisfied[9]

$$|E_A'(M, m+1) - E_A'(M, m)| \leqslant {}^1/_2 h(\Delta\nu)_B, \quad (5)$$

$$[T_{AB}^{(\pm)m,m+1}]^{-1} \gg T_A^{-1}(m, \mathbf{H}_0), T_B^{-1}(\mathbf{H}_0), \quad (6)$$

and ensure, together with (4), an effective thermal contact between the spins of the Ce^{3+} and the nuclear spins of Co^{59} with participation of all the hyperfine sublevels of the cobalt. In (5) and (6), $(\Delta\nu)_B$ is the width of the EPR line of Ce^{3+} in the field $\mathbf{H}_0$, and $[T_{AB}^{(\pm)m,m+1}]^{-1}$ are the rates of the ENCR transitions.[9] In a direction perpendicular to the vector $\mathbf{H}_0$ and to the C_3 axis, a pulsed magnetic field $\mathbf{H}_\perp^p(t)$ is applied (Fig. 1a) for the purpose of cooling the Ce^{3+} spins by adiabatic demagnetization. The duration of the pulse and its amplitude must be large enough for the spin system of Ce^{3+} to manage, in the region of the maximum values of the combined field $\mathbf{H}_\Sigma = \mathbf{H}_0 + H_\perp^p(t)$, to go into equilibrium with the lattice. In this case the pulse decay should be fast enough compared with time $T_B(\mathbf{H}_\Sigma)$ of the SLR of Ce^{3+}. After the termination of the $\mathbf{H}_\perp^p(t)$ pulse, the aforementioned thermal contact between the spin systems is re-established and they become thermally mixed. If the densities n_A and n_B of the Co^{2+} and Ce^{3+} satisfy the relation[9]

$$n_A \ll n_B, \quad (7)$$

the thermal mixing causes the reservoir of the hyperfine interactions of Co^{2+} to assume a low temperature T_I close to the temperature T_J of the cooled Ce^{3+} spins, and a short-duration nonequilibrium distribution of the populations takes place in the subsystem of the cobalt sublevels and is described by the formula[9]

$$n(M, m) \approx \frac{n_A \exp(-\delta M/kT_S - AMm/kT_I) \operatorname{sh}(A/4kT_I)}{2 \operatorname{ch}(\delta/2kT_S) \operatorname{sh}[A(2I+1)/4kT_I]}, \quad (8)$$

where the temperatures T_S and T_A are connected by the relation $T_L \gtrsim T_S > T_I \approx T_J$. It follows from (8) that at a sufficiently large gap between T_S and T_I, population inversion sets in and the maser effect becomes possible on the transitions $1/2, m \leftrightarrow -1/2, m$ with number $m < 0$ satisfying the relation (Ref. 9)[1)]

$$-Am/T_I > \delta/T_S. \quad (9)$$

The distribution (8) under the condition (9) is shown schematically in Fig. 1b.

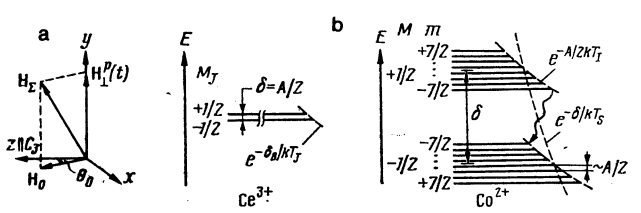

Fig. 1.a) Geometry of excitation of a spin system with the aid of a pulsed magnetic field $\mathbf{H}_\perp^p(t)$; x, y, z—crystal axes; b) distribution of populations of the energy levels of the ions Ce^{3+} and Co^{2+}, produced after turning off the field $\mathbf{H}_\perp^p(t)$ as a result of thermal mixing of the spin subsystems ($T_I \approx T_J$).

2. EXPERIMENT

We investigated an LaMN crystal with respective Co^{2+} and Ce^{3+} densities 0.1 and 3 at.% in the growth solution. These densities were chosen to satisfy the requirements (5)–(7). The fact that the set of condition (4)–(7) is simultaneously satisfied was confirmed in preliminary experiments by the rapid shortening of the relaxation time of Co^{2+}, observed by the pulsed saturation method, in the vicinity of the angle $\theta \approx \theta_0$. This shortening, due to the rapid redistribution (via the Ce^{3+} spins) of the excitation energy between the saturated transition $1/2, m \leftrightarrow -1/2$ m and the remaining hfs transitions of Co^{2+}, was observed only for the X centers of Co^{2+} (at $\theta \approx 1°$).[2)]

The nonequilibrium states of the Co^{2+} spins were investigated at a crystal temperature $T_L = 1.7$ K, using a superheterodyne EPR spectrometer at a fixed frequency $\nu = 9.1$ GHz. The sample was placed near the lower wall of the rectrangular microwave cavity in the TEM_{102} mode and subjected to the action of two homogeneous magnetic fields, stationary $\mathbf{H}$ whose direction could be varied in the horizontal plane (the xz plane in Fig. 1a), and vertical pulsed field $\mathbf{H}_\perp^p(t)$. The latter was produced by a procedure close to that described in Ref. 17, using controlled discharge of a capacitor bank through a copper-wire solenoid ($L \approx 40$ mH). The solenoid was pressed into the foamed-plastic nitrogen vessel of the cryostat (the helium vessel was made of glass). When the temperature was lowered to 77 K, the active resistance of the solenoid decreased by ≈ 7 times and the discharge became oscillatory. A thyristor switching system produced in the solenoid isolated current pulses of duration τ_p, which were approximated with good accuracy by the function

$$i(t) = i_0 \exp[-\gamma(t+\tau_p)] \sin[(t+\tau_p)\pi/\tau_p]$$

$$(-\tau_p \leqslant t \leqslant 0, \quad i_0 = \text{const}) \quad (10)$$

with parameters $\tau_p = 35$ msec and $\gamma = 0.033$ msec^{-1}. At $i_0 = 100$ A, the amplitude $H_{\max}$ of the field $\mathbf{H}_\perp^p(t)$ was approximately 10 kOe. Owing to the strong field dependence of the SLR rate of the Kramers ions ($T_1^{-1} \sim H^4$, Ref. 14), the field $\mathbf{H}_\perp^p(t)$ produced by the current (10) satisfied quite fully,

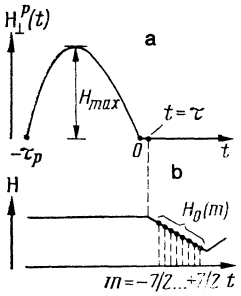

Fig. 2. Scheme of spectral measurements: a) Exciting-magnetic-field pulse; b) change of stationary magnetic field with time ($t = \tau$ is the initial instant of observation).

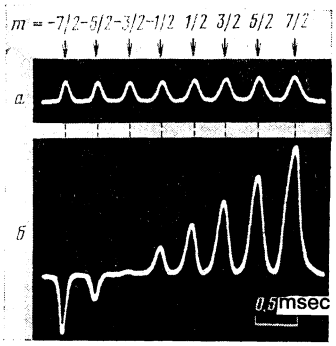

Fig. 3. Oscillograms of the EPR spectra of Co^{2+} ions: a) at a thermal equilibrium with the/lattice; b) under conditions of thermal excitation of the spin system.

at sufficiently high amplitudes, the requirements formulated above.

To prevent excessive heating of the microwave-cavity walls by the eddy currents induced by the pulsed fields, the following measures were taken. The cavity was made of foil-clad glass-cloth-based laminate; narrow slots were cut in the foil of the lower and broad lateral walls of the cavity, to break up the long eddy-current lines. The sample was separated from the mounting wall by thermal-insulation glass plate.

The action of the field H on the pulsed current caused a torque to be applied to the solenoid and produce kicks in the measuring system. The solenoid-holding vessel was therefore firmly secured between the polepieces of the main magnet.

It is known[13,14] that at $T_L \lesssim 2$ K the SLR of Ce^{3+} ions in an LaMN lattice can be accompanied by a phonon bottleneck. To weaken the possible influence of this factor on the investigated processes, a thin layer of vacuum grease was coated on the surface of the sample, thus ensuring its acoustic matching to the surrounding liquid helium.

We investigated in the experiment the non equilibirum EPR spectrum and the kinetics of the allowed transitions of the Co^{2+} ions under conditions when the spin system was excited by a pulsed magnetic field. All but the angle measurement were performed at fixed orientations of the fields **H** and $\mathbf{H}_1^p(t)$ relative to the crystal axes, as shown in Fig. 1a. The spectral observations were performed in the following manner (Fig. 2). The field **H** was oriented at an angle $\theta \approx \theta_0$ to the C_3 axis, and its intensity exceeded somewhat the resonant value $H_0(-7/2)$ for the transition $1/2, -7/2 \leftrightarrow -1.2, -7/2$. The field $\mathbf{H}_1^p(t)$ was turned on next. After the termination of the magnetic pulse (instant of time $t = 0$), at a time $\tau \approx 1.5$ msec, the scanning of the field **H** was started in the direction of lower intensities; at the same time, the oscilloscope sweep was turned on and the EPR spectrum was observed. The delay time τ was chosen such that maximum inversion was observed in the transition with $m = -7/2$. The procedure for observing the kinetics of the EPR signals differed from that described in that the field H remained constant and equal to the resonant value $H_0(m)$ for the chosen transition, while the oscilloscope sweep was turned on barely prior to the instant $t = 0$. All the measurements were performed on the conditions far from EPR saturation; this ensured linear reproducibility of the signals.

The EPR spectra obtained for the Co^{2+} ions, under the conditions of thermal equilibrium and upon excitation of the spin system by a pulsed field with $H_{max} = 10$ kOe, are shown in Fig. 3a and 3b. It can be seen that the two strong-field lines on Fig. 3b are inverted, and the maximum inversion coefficients k_m are $k_{-7/2} \approx 3.2$ and $k_{-5/2} \approx 1.3$. The form of the envelope of the spectral lines agrees qualitatively with the distribution (8). With decreasing amplitude H_{max}, the deviation of the observed spectrum from the equilibrium value decreased correspondingly. For the transition with $m = -7/2$, inversion vanished at $H_{max} \approx 4$ kOe.

Figure 4 shows oscillograms of the EPR spectra, which describe the kinetics of the tansitions with $m = -7/2$ and $m = 5/2$, as well as the analytic curve that illustrates the real process occurring in the transition with $m = -7/2$. We consider the latter together with the experimental curves *a* and *b*. The point *A* on this curve corresponds to the start of passage through the spectral line. Since $H = H_0$ ($m = -7/2$), and the rate of change of the field $\mathbf{H}_1^p(t)$ at the end of the pulse is high, half the contour of the spectral line is scanned even before the start of the thermal mixing (segement A–*B*; it cannot be seen on the experimental curve *b* because of the relatively high velocity of the beam). As a result of magnetic cooling of the electron spins of the cobalt (see footnote 1), the point *B* turns out to be higher than the level of the thermal equilibrium of the absorption. This is followed by a rapid thermal mixing, as a result of which maximum inversion is reached (segment *B*–*C*); the duration of this stage is determined by the rates of the ENCR. The next stage is a relatively slow change of the function, with a duration determined by the rates of the electronic SLR of the ions of both types. If $T_A^{-1}(m) < T_B^{-1}$, the process should evolve beyond the point *C* in qualitative accordance with the dashed curve of Fig. 4b. In the case $T_A^{-1}(m) < T_B^{-1}$, the curve passes through a point *D* that lies above the level of the equilibrium absorption. It can be seen from Fig. 4b that the latter variant is realized in the experiment. The lifetime τ_I of the inversion on the transition with $m = -7/2$ is 36 msec.

To obtain the oscillograms of the kinetic curves, the oscilloscope beam sweep was turned on shortly before the end of the $\mathbf{H}_1^p(t)$ pulse, in order that the EPR line be observed on the transition $1/2, m-1 \leftrightarrow -1/2, m-1$, which is the neighbor of the observation transition $1/2, m-1 \leftrightarrow -1/2$ *m*. In Fig. 4c the corresponding spectral line ($m - 1 = 3/2$) is prepresented by a narrow upward peak at the start of the curve. The measurement of the amplitudes of such spectral lines from oscillograms obtained for all the allowed transitions makes it possible to establish the distribution of the

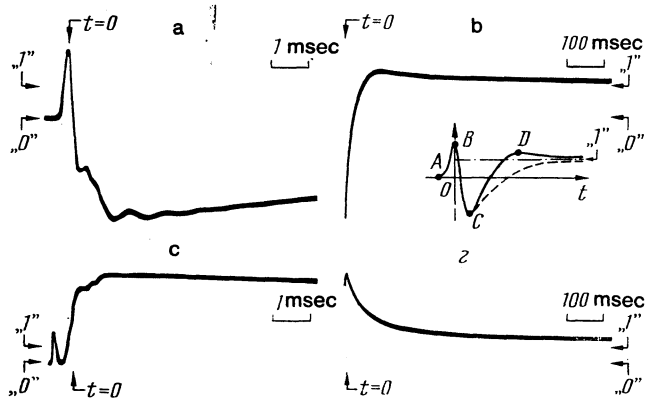

Fig. 4. Oscillograms of the signals of the kinetics of EPR of Co^{2+} ions under thermal excitation of the spin system. a, b) The transition 1/2, − 7/2↔ − 1/2, − 7/2 (in the lower corner of Fig. b shows the analytic curve); c, d) the transition 1/2, 5/2↔ − 1/2, 5/2 ("0" and "1" are the levels of the zero and thermal-equilibrium absorption).

populations of the spin sublevels of Co^{2+} directly before the start of the thermal mixing.

The small-scale fluctuations that can be noted on the experimental curves 4a, 4c, and 6a and vanish in the course of time are not connected with the precesses occurring in the sample. They can be attributed to the residual influence, of the aforementioned thermal and mechanical factors of magnetic origin, on the natural frequency of the microwave cavity and on the degree of its coupling with the waveguide channel.

Figure 5 shows the experimental angular dependence of the quantity $k_{-7/2}$, obtained from spectral measurements in which the line with $m = k_{-7/2}$ was passed at the instant of time $t = 2$ msec. This plot reflects only approximately the dependence of the effect on the angle θ, owing to the inaccuracy in the setting of the sample relative to the horizontal plane (the angle α between the axis $z \| C_3$ and this plane did not exceed 1°). It can be seen that at a value $|\phi| \approx 1°$ close to the calculated value $\phi_0 = 1.32°$ the inversion has a maximum, thus confirming the resonant character of the thermal contact of the spin systems.

3. KINETIC EQUATIONS

To interpret the experimental kinetic dependences, we used the following system of approximate balance equations for the relative (per ion) populations $\tilde{n}(M,m)$ and $\tilde{n}_B(M_J)$ of the spin sublevels of Co^{2+} and Ce^{3+}

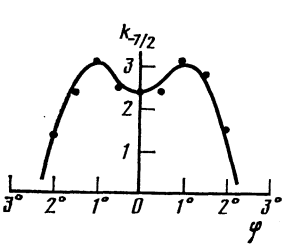

Fig. 5. Angular dependence of the maximum inversion coefficient on a transition with $m = -1/2$ for the instant of time $t = 2$ msec (ϕ is the angle between the vector **H** and the projection of the C_3 axis on the horizontal plane, $\cos\theta = \cos\alpha\cos\beta$): points—experiments; curves—calculation at $|\alpha| = 0.87°$, $(\Delta\nu)_B = 26$ MHz.

$$\frac{d\tilde{n}(\pm 1/2, m)}{dt} = -\tilde{n}(\pm 1/2, m) W^{A}_{\pm 1/2, \mp 1/2}(m) + \tilde{n}(\mp 1/2, m) \times W^{A}_{\mp 1/2, \pm 1/2}(m) + U^{\pm}_{m,m+1} + U^{\pm}_{m,m-1}, \quad (11)$$

$$\frac{d\tilde{n}_B(1/2)}{dt} = -\tilde{n}_B(1/2) W^{B}_{1/2,-1/2} + \tilde{n}_B(-1/2) W^{B}_{-1/2,1/2} + \frac{n_A}{n_B}\left(\sum_{m=-I}^{I-1} U^{+}_{m,m+1} + \sum_{m=-I+1}^{I} U^{-}_{m,m-1} \right), \quad (12)$$

$$U^{\pm}_{m,m+1} = \left(\frac{n_B}{n_A + n_B}\right) [T_{AB}^{(\pm)m,m+1}]^{-1} \times [\tilde{n}(\pm 1/2, m+1)\tilde{n}_B(\mp 1/2) - \tilde{n}(\pm 1/2, m)\tilde{n}_B(\pm 1/2)],$$

$$U^{\pm}_{m,m-1} = \left(\frac{n_B}{n_A + n_B}\right) [T_{AB}^{(\pm)m,m-1}]^{-1} \times [\tilde{n}(\pm 1/2, m-1)\tilde{n}_B(\pm 1/2) - \tilde{n}(\pm 1/2, m)\tilde{n}_B(\mp 1/2)], \quad (13)$$

$$\sum_{M,m} \tilde{n}(M,m) = 1, \quad \tilde{n}_B(1/2) + \tilde{n}_B(-1/2) = 1, \quad \tilde{n}_B(1/2)/\tilde{n}_B(-1/2) = \exp(-\delta_B/kT_J).$$

In (11) and (12), the probabilities

$$W^{A}_{-1/2,1/2}(m) = T_A^{-1}(m) \frac{\exp(-h\nu_m/2kT_L)}{2\operatorname{ch}(h\nu_m/2kT_L)},$$

$$W^{A}_{1/2,-1/2}(m) = T_A^{-1}(m) - W^{A}_{-1/2,1/2}(m), \quad (14)$$

$$W^{B}_{-1/2,1/2} = T_B^{-1} \frac{\exp(-h\nu_B/2kT_L)}{2\operatorname{ch}(h\nu_B/2kT_L)}, \quad W^{B}_{1/2,-1/2} = T_B^{-1} - W^{B}_{-1/2,1/2}$$

characterize the electronic SLR of the ions Co^{2+} and Ce^{3+}, respectively ($h\nu_m = \delta + Am$, $h\nu_B = \delta_B$). The rates of the ENCR are equal to[9]

$$[T_{AB}^{(\pm)m,m+1}]^{-1} = \frac{n_A + n_B}{n_A n_B V} \sum_{i,j} [w_{cr}^{(\pm)m,m+1}]_{ij}^{-1} = V_{cr}^{\pm} I_m \Phi_m^{\pm}. \quad (15)$$

The $\pm$ signs correspond here to the states $M = \pm 1/2$ of cobalt, V is the volume of the crystal, and $I_m = I(I+1) - m(m+1)$. The probabilities $[W_{cr}^{(\pm)m,m+1}]_{ij}^{-1}$ of the two-particle ENCR transitions are defined by the expressions[9,14,15,17]

$$[w_{cr}^{(+)m,m+1}]_{ij}^{-1} = \frac{(1 - 3\cos^2\theta_{ij})^2 Q^{+} I_m \Phi_m^{+}}{r_{ij}^6},$$

$$[w_{cr}^{(-)m,m+1}]_{ij}^{-1} = \frac{9Q^{-} I_m \Phi_m^{-} \sin^4\theta_{ij}}{r_{ij}^6},$$

$$Q^{\pm} = \frac{(g_{\perp}^{B})^2 \beta^2 (g_{\perp}^{N} \beta_N \pm A_{\perp} g_{\perp}^{A} \beta/2\delta)^2}{16\sqrt{2\pi}\hbar^2 (\Delta\nu)_B},$$

$$\Phi_m^{\pm} = \exp\left[-\frac{(\nu^{\pm}_{m,m+1} - \nu_B)^2}{2(\Delta\nu)_B^2} \right], \quad (16)$$

$$\nu^{\pm}_{m,m+1} = \frac{1}{h} |E_A(\pm 1/2, m+1) - E_A(\pm 1/2, m)|,$$

$$[w_{cr}^{(\pm)m,m+1}]_{ij}^{-1} = [w_{cr}^{(\pm)m+1,m}]_{ij}^{-1}.$$

The summation in (15) is over all the ions Ce^{3+} and X-Co^{2+}. In (15) and (16) we took into account the direct dipole-dipole

interaction of the nuclear spin of the ith Co^{2+} ion with the spin of the jth Ce^{3+} ion, as well as the indirect interaction caused by the hyperfine and electronic dipole-dipole interactions of these ions; the latter predominates for the X centers of Co^{2+}. The EPR line shapes of Ce^{3+} at the frequency ν_B, and the NMR line shapes of Co^{59} at the frequencies $\nu^{\pm}_{m,m+1}$, are assumed to be Gaussians with widths corresponding to the condition $\Delta\nu_{m,m+1} \ll (\Delta\nu)_B$.[18]

Equations (11)–(13) are generalizations of the equations of Ref. 9, written for $I = 1/2$, to include the case of arbitrary nuclear spin I.

4. ANALYSIS OF EXPERIMENTAL RESULTS

The analysis of the the kinetics of the system was based on Eqs. (11)–(13), which were solved with a computer by the Runge-Kutta method under the following initial conditions and assumptions.

The rates $P_A^{-1}(m)$ of the SLR in (14) were determined from the formula ($\mathbf{H} \| C_3$)

$$T_A^{-1}(m) = C\left\{H + q\left[m - \frac{A_\perp (I^2+I-m^2)}{2h\nu_m}\right]\right\}^2 \nu_m^3 \operatorname{cth}\frac{h\nu_m}{2kT_L}, \tag{17}$$

which was obtained by simple calculation in accordance with the scheme of Ref. 14 (see also Ref. 16). The phenomenological constants $C = 0.38\cdot10^{-36}$ $\text{sec}^{-1}\cdot\text{Oe}^{-2}\cdot\text{Hz}^{-3}$ and $Q = 167$ Oe were obtained from the aforementioned relaxation measurement on an LaMN:Co^{2+} (0.1 at.%) crystal.[3)]

The calculations were made using the foregoing values of the parameters of the spin Hamiltonians (1) and (3) at $\nu = 9.1$ GHz, $T_L = 1.7$ K, $n_a/n_b = 1/30$,[4)] and $\theta = \theta_0 = 1.32°$. the parameter ratio V_{cr}^+/V_{cr}^- was assumed to be 1/6. This value was obtained from (15) and (16) by replacing the expressions for $(1-3\cos^2\theta_{ij})^2$ and $\sin^4\theta_{ij}$ by values averaged over a sphere. The parameters $\delta/2kT_S^0 = X_A^0, T_I^0$, and $\delta_B/2kT_J^0 = X_B^0$, which specify in accordance with (8) and (13) the initial distribution of the populations in the spin system after the end of the demagnetization (for the instant of time $t = 0$), and also V_{cr}^-, T_B^{-1}, and $(\Delta\nu)_B$ were regarded as subject to determination.

In the course of the computer calculations we determined the functions

$$F(m) = [\tilde{n}(-1/2, m) - \tilde{n}(1/2, m)]/\Delta\tilde{n}_L(-I), \tag{18}$$

where

$$\Delta\tilde{n}_L(-I) = \frac{1}{2I+1}\frac{\operatorname{sh}[(\delta - AI)/2kT_L]}{\operatorname{ch}(\delta/2kT_L)} \tag{19}$$

is the thermal-equilibrium value of the difference between the relative populations on the transition with $m = -I$. The sought parameters [with the exception of $(\Delta\nu)_B$] were fitted together by comparing the functions $F(m)$ with the experimental kinetic curves; in this case the parameters X_A^0 and X_B^0 were fitted to the maxima of the signals of the induced radiation on Fig. 4a and absorption on Fig. 4b and 6a, while the parameters V_{cr}^- and T_E^{-1} were fitted in accord with the segements B–C and C–D of curves Fig. 4a and 4b, respectively; finally, $(\Delta\nu)_B$ were fitted to the experimental angular dependence of $k_{-7/2}$ (Fig. 5). In the latter case it was assumed

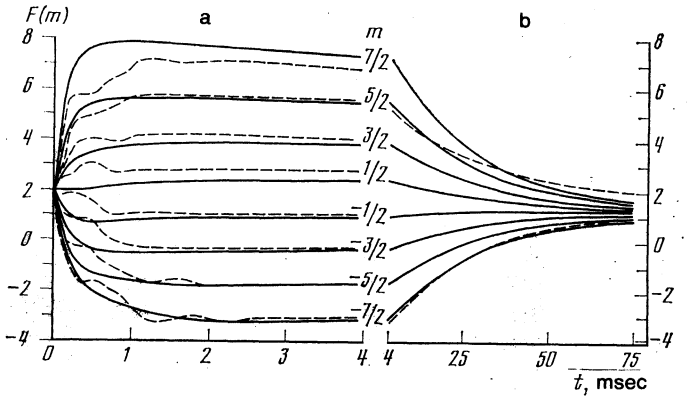

Fig. 6. Kinetics of relative difference of the populations of the spin sublevels of Co^{2+} on the transitions 1/2, $m \leftrightarrow -1/2$, m as function of m: a) stage of thermal mixing; b) stage of return to equilibrium; solid curve—calculation; dashed—experiment.

in addition that the maximum inversion on the experimental curve (Fig. 5) at $|\phi| \approx 1°$ corresponds to an angle $\theta = 1.32°$, i.e., $|\alpha| \approx 0.86°$. The possibility of separately varying the parameters in the indicated sequence and convergence of the adjustment process, which were carried out cyclically, were due to reliable statisfaction of condition (6).

The calculations yielded the following values:

$$X_A^0 = 0.25 \pm 0.015 \quad (T_S^0(m = -7/2) = 0.95 \mp 0.05 \text{ K}),$$

$$T_I^0 = -1.2 \mp 0{,}25 \text{ K},$$

$$X_B^0 = 0.19 \pm 0.01 \quad (T_J^0 = 0.015 \mp 0.001 \text{ K}),$$

$$V_{cr}^- = 5500 \pm 1100 \text{ sec}^{-1},$$

$T_B^{-1} = 31 \pm 4$ sec^{-1}, and $(\Delta\nu)_B = 26 \pm 6$ MHz.[5)] The corresponding plots of the functions $F(m)$ are shown in Fig. 6, which contains also for comparison the experimental curves. It can be seen that on the whole the calculated dependences are in fair agreement with the experimental ones. Let us discuss the most significant discrepancies and accordingly the question of the accuracy of the calculated parameters.

The nonmonotonic character of the experimental curves (Figs. 4, 6a) during the stage of thermal mixing, and the error in specifying the angel θ, affected substantially the accuracy of the determination of only the parameters $V_{cr}^{\pm}$. In the time region $t \gtrsim 30$ msec, the agreement between the experimental and theoretical plots for $m \geqslant 3/2$ becomes worse, as can be seen with the curve for $m = 5/2$ as the example (Fig. 6b). The most probable reason is the approximate character of the description of the SLR of Co^{2+} with the aid of Eq. (7) (no account was taken of "oblique" relaxation transitions[16]).

The foregoing calculations of T_S^0 and T_I^0 practically coincide with the temperatures obtained from the amplitudes of the spectral lines (see Fig. 4) on all the allowed transitions. Knowing the values of T_S^0 and $k^{-7/2} \approx 3.2$ we can determine with the aid of (8) the temperature T_I which is reached as a result of thermal mixing, namely $T_I \approx 0.028$ K. Substituting the values of T_I and T_I^0 into the equation

$$\mathrm{th}\,(A/4kT_J^0)+\frac{n_A}{n_B}\{(2I+1)\,\mathrm{cth}[A(2I+1)/4kT_I^0]-\mathrm{cth}\,(A/4kT_I^0)\}$$
$$=\mathrm{th}(A/4kT_I)+\frac{n_A}{n_B}\{(2I+1)\,\mathrm{cth}[A(2I+1)/4kT_I]-\mathrm{cth}(A/4kT_I)\}, \quad (20)$$

which follows from the condition that the thermal mixing process be adiabatic (at $\delta_B = A/2$), we obtain $T_J^0 \approx 0.016$ K, which is very close to the value given above.

It is of interest to note that the temperature T_S^0 and T_I can also be determined by a simpler albeit not so accurate a method, namely by approximating the spectrum on Fig. 3b, on the basis of the distribution (8), from the minimum of the sum of the squares of the differences between the calculated and experimental values of the relative amplitudes of the *hfs* components. From the known value of T_I, putting in (20) $T_I^0 = \infty$ (which is perfectly admissible by virtue of (7)), we can obtain also T_J^0. The temperatures $T_S^0(m = -7/2) = 0.87 \pm 0.05\,K$, $T_I = 0.03 \pm 0.015$ K, and $T_J^0 \approx 0.018$ K are close enough to those obtained earlier.

5. DISCUSSION

We consider the basic maser characteristics of the system. For the transition with $m = -7/2$ the magnetic Q_M of the working crystal can be written in the form

$$\frac{1}{Q_M} = \frac{\pi (g_\perp^A)^2 \beta^2 n_A k_{-7/2} \Delta\tilde{n}_L(-7/2)\,\eta}{2\hbar(\Delta\nu)_A}. \quad (21)$$

Here η is the cavity filling factor, $(\Delta\nu)_A \approx 90$ MHz is the width of a separate component of hfs in the EPR spectrum of Co^{2+}. At $T_L = 1.7$ K, $K_{-7/2} = 3.2$, $\nu = 9.1$ GHz, $n_A = 1.6 \cdot 10^{18}$ cm^{-3} (0.1 at.% Co^{2+}), and $\eta = 1$ we obtain $Q_M \approx 400$, which is only four times worse compared with the typical value $Q_M = 100$ for a maser ruby. It is now the purpose of the present study to investigate the density dependence of the maser effect, and it can be assumed that for the realized excitation conditions the presented value of Q_M is not the best. In addition, there are no grounds for assuming the form, amplitude, and duration of the realized pulse (10) to be optimal.

The lifetime τ_J of the inversion is determined by the temperatures T_S^0 and T_J^0 in (8) and (20) as well as by the rates of the SLR of the ions of both sorts; at $n_A \ll n_B$ it depends to the greatest degree on $T_B^{-1.9}$. For Kramers ions in the region of small splittings δ_B one should expect a strong concentration dependence of $T_B(n_B)$.[20] Thus, the parameters Q_M and τ_I can be improved both by choosing optimal densities n_A and n_B, and by increasing the amplitudes of the exciting pulse and optimizing its wave form. A considerable gain of Q_M can be expected also for similar objects such as $^{161}Dy^{3+}$: Ce^{3+}: LaMN (Ref. 14) or yttrium ethyl sulfate (YES) doped with $^{167}Er^{3+}$ and also with D_y^{3+} or Yb^{3+},[17,21] where the role of the centers of sort A is assigned respectively to the ions $^{161}Dy^{3+}$ and $^{167}Er^{3+}$, which have large g factors and large I [the latter is convenient in the sense of (9)].

In systems with $|g_\perp^B| > |g_\parallel^B|$ the working frequency of the maser cannot substantially exceed the value $\nu_{\max}^{-I}$ which is realized at $\theta_0 = 0°$ in (4):

$$\nu_{-I}^{\max} = \frac{|A_\parallel|}{h}\left(\frac{|g_\parallel^A|}{2|g_\parallel^B|} - I\right). \quad (22)$$

For the crystal investigated, $\nu_{\max}^{-I} = 19.6$ GHz. If, however, $|g_\perp^B| < |g_\parallel^B|$ it is necessary to replace in (22) $A_\parallel$, $g_\parallel^A$, and $g_\parallel^B$ by $A_\perp$, $g_\perp^A$, and $g_\perp^B$, respectively; in this case $\theta_0 = 90°$. For example, for $^{167}Er^{3+}$: Yb^{3+}: YES we have $g_\perp^B \approx 0.0084$ (Ref. 21), $g_\perp^A = 8.78$, and $A_\perp = 0.0311$ cm^{-1} (Ref. 22), which yields $\nu_{-I}^{\max} \approx 484$ GHz. We note, however, that depending on the experimental conditions, relations (5), (6), and (9) can impose stronger restrictions on the limiting frequency than (22).

Systems similar to the investigated one are not restricted to the objects named above. By way of additional examples we can name $^{59}Co^{2+}$: Ti^{3+}: Al_2O_3, as well as Yb^{3+}: $YCl_3 \cdot 6H_2O$ with $^{161,163}Dy^{3+}$ or $^{167}ER^{3+}$ impurity.[14,21]

Our investigation proves the feasibility of realizing in a paramagnetic crystal direct conversion of the energy of thermal phonons into the energy of coherent microwave radiation. Just as for GDL, the concept of a quantum heat engine[8] is applicable to this system. The heater and cooler are respectively the crystal lattice in contact with the liquid helium, and the system of cooled cerium spins. The coherent radiation is the analog of the mechanical work. In the spin system of cobalt, which performs the functions of the working medium with discrete energy spectrum, a cyclic process[10] similar to the Carnot cycle takes place.

In light of the foregoing, it is of interest to realize maser systems[23] intended for work in a stationary regime. They differ from the considered system by the method of polarization of spins of type B, for which it is proposed to use microwave pumping. The amplification should be effected as before on the basis of the distribution (8) on account of the energy of the thermal phonons; this apparently makes it possible to obtain definite practical advantages over the known schemes of stationary microwave masers.[6)]

There is a deep analogy between nonequilibrium states in the studied system described by the distribution (8), and the spin-system states that are observed in experiments on not-strictly-resonant saturation of EPR.[24] In both cases partial inversion is achieved by the temperature difference between relatively weakly coupled spin subsystems, but in the system discussed here the inversion is characterized by a much larger inversion coefficient and is due to the mechanism of thermal mixing of nuclear spins of the ions of one sort with previously polarized electron spins of the ions of the other sort. This mechanism is similar in basic features with the mechanism of polarization of nuclei in experiments on the spin refrigerator.[12,17,21] It is obvious from the foregoing that the results of the present paper are outside the scope of quantum electronics and can be of methodological interest for the investigation of the dynamics and kinetics of complicated spin systems in paramagnetic crystals.

The authors are grateful to the late Corresponding Member of the USSR Academy of Sciences S. A. Al'tshuler for support.

[1)]The relation $T_L \gtrsim T_S$ reflects the possibility of a certain lowering [undesirable by virtue of (9)] of the electron spin temperature T_S of cobalt as a result of the rapid decay of the pulsed field.

[2)]When referring to Co^{2+} ions we imply herafter only their X centers.
[3)]Measurements have shown that in a given n_A the cross relaxation processes in the *hfs* transition system[14,16] no longer appear.
[4)]The indicated value of n_A/n_B was obtained under the assumption that the densities of the ions in the crystal and in the growth solution are equal and that only 2/3 of the total number of cobalt ions occupy the X position.[19]
[5)]Owing to the high rate of change of the pulsed fields in the final segment of the decay, the parameters X_A^0 and X_B^0 are practically independent of either the angle θ (in the interval $|\theta| \lesssim 2.5°$ of interest) or the number m of the observation that characterizes the transition. Dependent on θ and m, however, are the splittings δ and δ_B, and this leads to a corresponding dependence of the temperatures T_S^0 and T_J^0. For the Y centers of Co^{2+}, owing to the smallness of $A_\perp \leqslant 0.0003$ cm^{-1} (Ref. 9), the corresponding values of $V_{cr}^{\pm}$ turn out, as can be seen from (15) and (16), smaller by a factor ≈ 4500 than for the X centers. The condition (6) is then relatively well satisfied with respect to the rates $T_A^{-1}(m)$ (Ref. 9), but is not satisfied with respect to T_B^{-1}, and it is this which caused the negative result of the experiments with Y centers at the employed cerium-ion density n_B.
[6)]If, for example, the effects of spin J of donors of type B is equal to unity and the Hamiltonian $\mathscr{H}_B$ (3) contains an additional terms in the form $-|D|(J_Z^2 - 2/3)$, the microwave pumping should be carried out in the orientation $\mathbf{H}\|z$ on the transition $-1 \leftrightarrow 0$ in fields $H_\pm = (|D| \pm A_\parallel/2)/g_\parallel^B\beta$.

[1]E. O. Schulz-Dubois and H. E. D. Scovil, in: Quantum Electronics (a symposium), N. Y. Columbia Univ. Press, 1960, p. 217.
[2]H. E. D. Scovil and E. O. Schulz-Du Bois, Phys. Rev. Lett. **2**, 262 (1959).
[3]E. O. Schulz-Du Bois and H. E. D. Scovil, US Patent No. 3015072, Priority 26 Dec. 1961.
[4]V. K. Konyukhov and A. M. Prokhorov, Usp. Fiz. Nauk **119**, 541 (1976) [Sov. Phys. Usp. **19**, 618 (1977)].
[5]N. G. Basov and A. N. Oraevskii, Zh. Eksp. Teor. Fiz. **44**, 1742 (1963) [Sov. Phys. JETP **17**, 1171 (1963)].
[6]V. K. Monyukhov and A. M. Prokhorov, Pis'ma Zh. Eksp. Teor. Fiz. **3**, 436 (1966) [JETP Lett. **3**, 286 (1966)].
[7]N. G. Basov, A. N. Oraevskiĭ, and B. A. Shcheglov, Zh. Tekh. Fiz. **37**, 339 (1967) [Sov. Phys. Tech. Phys. **12**, 243 (1067)].
[8]J. E. Geusic, D. O. Schulz-Du Bois, and H. E. D. Scovil, Phys. Rev. **156**, 353 (1967).
[9]M. P. Vaĭsfel'd, Fiz. Tverd. Tela (Leningrad) **20**, 124 (1978) [Sov. Phys. Solid State **20**, 67 (1978)].
[10]M. P. Vaĭsfel'd, in: Magnetic Resonance and Related Phenomena (Proc. 20th Congress Ampere, Talinn, 21-26 August, 1978). Springer, 1979, p. 334.
[11]M. P. Vaĭsfel'd, F. S. Imamutdinov, and A. Kh. Khasanov, Pis'ma Zh. Eksp. Teor. Fiz. **34**, 252 (1981) [JETP Lett. **34**, 240 (1981)].
[12]L. Niesen and W. J. Huiskamp, Physica **57**, 1 (1972).
[13]A. Abragam and B. Bleaney, Electron Paramagnetic Resoanance of Transition Ions, Oxford, 1970.
[14]S. A. Al'tshuler and B. M. Kozyrev, Electron Paramagnetic Resonance of Intermediate-Group Elements [in Russian], Nauka, 1972.
[15]J. Lubbers and W. J. Hiskamp, Physica **34**, 193 (1967).
[16]W. P. Unruh and J. W. Culvahouse, Phys. Rev. **129**, 2441 (1963).
[17]J. R. McColl and C. D. Jeffries, Phys. Rev. **B1**, 2917 (1970).
[18]S. H. Choh and G. Seidel, Phys. Rev. **164**, 412 (1967).
[19]J. A. Roest *et al.*, Physica **64**, 335 (1973).
[20]N. E. Kask, Fiz. Tverd. Tela (Leningrad) **8**, 1129 (1966) [Sov. Phys.-Solid State **8**, 900 (1966)].
[21]H. B. Brom and W. J. Hiuskamp, Physica **66**, 43 (1978).
[22]H. J. Stapleton, R. L. Marchand, and F. R. Lemar, Phys. Rev. **B10**, 2687 (1974).
[23]M. P. Vaĭsfel'd, Abstracts, 9th All-Union Conf. on Incoherenta and Nonlinear Optics, M. 1978, partl, p. 33.
[24]V. A. Atsarkin and M. I. Rodak, Usp. Fiz. Nauk 167, 3 (1972) [Sov. Phys. Usp. **15**, 251 (1972)].

Translated by J. G. Adashko